GCN-LSTM Based Transient Angle Stability Assessment Method for Future Power Systems Considering Spatial-temporal Disturbance Response Characteristics

Shiwei Xia, *Senior Member*, *IEEE*, Chenhui Zhang, Yahan Li, Gengyin Li, *Member*, *IEEE*, Linlin Ma, Ning Zhou, Ziqing Zhu, *Member*, *IEEE*, and Huan Ma

***Abstract*—Traditional transient angle stability analysis methods do not fully consider the spatial characteristics of the network topology and the temporal characteristics of the time-series disturbance. Hence, a data-driven method is proposed in this study, combining graph convolution network and long short-term memory network (GCN–LSTM) to analyze the transient power angle stability by exploring the spatiotemporal disturbance characteristics of future power systems with high penetration of renewable energy sources (wind and solar energy) and power electronics. The key time-series electrical state quantities are considered as the initial input feature quantities and normalized using the Z-score, whereas the network adjacency matrix is constructed according to the system network topology. The normalized feature quantities and network adjacency matrix were used as the inputs of the GCN to obtain the spatial features, reflecting changes in the network topology. Subsequently, the spatial features are inputted into the LSTM network to obtain the temporal features, reflecting dynamic changes in the transient power angle of the generators. Finally, the spatiotemporal features are fused through a fully connected network to analyze the transient power angle stability of future power systems, and the softmax activation cross-entropy loss functions are used to predict the stability of the samples. The proposed transient power angle stability assessment method is tested on a 500 kV AC-DC practical power system, and the simulation results show that the proposed method could effectively mine the spatiotemporal disturbance characteristics of power systems. Moreover, the proposed model has higher accuracy, higher recall rate, and shorter training and testing times than traditional transient power angle stability algorithms.**

***Index Terms*—Future power system, spatiotemporal disturbance characteristics, transient power angle stability, graph convolutional network, long short-term memory network.**

I. Introduction

Due to large disturbances, transient power angle stability problems are likely to occur with an increase in the development of renewable energy systems and complex network topologies. With these advances, power systems exhibit apparent spatiotemporal characteristics during dynamic transients. However, traditional transient power angle stability assessment methods do not fully consider changes in the spatial characteristics of the network topology and changes in the temporal characteristics of the electrical state quantities [1]. Therefore, it is crucial to devise a transient power angle stability assessment method that considers the spatiotemporal disturbance characteristics of the power system.

At present, artificial intelligence technologies, such as machine learning and deep learning methods, are widely used in transient power angle stability evaluation of power systems. The machine learning methods [2]–[4] include support vector machines (SVMs), decision trees (DTs), and extreme gradient boosting (XGBoost). Deep learning methods [5]–[7] include convolutional neural networks (CNNs,) long short-term memory (LSTM) networks, and gated recurrent unit (GRU) networks. Reference [8] proposed that the relative power angle, bus voltage amplitude, and phase angle of the generators are time-series data with time-varying characteristics during transient stability. A bidirectional LSTM network stability assessment model was established to assess the transient power angle

Received: December 20, 2023
Accepted: July 26, 2024
Published Online: November 1, 2024

Shiwei Xia, Chenhui Zhang, Yahan Li, and Gengyin Li are with the School of Electrical and Electronic Engineering, North China Electric Power University, Beijing 102206, China (e-mail: s.w.xia@ncepu.edu.cn; 120222201704@ncepu.edu.cn; 13872585752@139.com; ligy@ncepu.edu.cn).

Linlin Ma is with the State Grid Shandong Dispatch and Control Center, Jinan 250003, China (e-mail: hosee@163.com).

Ning Zhou and Huan Ma are with the State Grid Shandong Electric Power Research Institute, Jinan 250001, China (e-mail: may187144341@163.com; mahuan_epri@126.com).

Ziqing Zhu (corresponding author) is with the Department of Computer Science, Hong Kong Baptist University, Hong Kong 999077, China (e-mail: ziqing-yancy.zhu@polyu.edu.hk).

DOI: 10.23919/PCMP.2023.000116

stability based on time-series characteristics. Reference [9] proposed a time-adaptive transient power angle stability interpretable assessment model based on GRU network, which was a two-stage mechanism consisting of feature and temporal attention blocks. Reference [10] used an improved one-dimensional convolutional neural network (1D-CNN) to develop a fast and accurate online stability assessment method, in which the convolutional layers were smartly determined by the type and characteristics of the input data to facilitate feature extraction. The aforementioned models consider the temporal characteristics of the electrical state quantities in the transient process and effectively evaluate the transient power angle stability of the power system. However, these models cannot excavate the spatial characteristics accompanied by changes in the network topology during the transient process and they do not consider the influence of the network topology on the transient power angle stability of the power system. Other studies have explored the spatial characteristics of the transient process of power systems. Reference [11] designed a multigraph attention network using an improved graph attention mechanism, which enhanced the adaptability of the assessment model to topological changes in the system. However, the temporal characteristics of the relative power angle of the generators during the transient process were not considered. Reference [1] developed a graph attention deep network assessment model that considered the adjacency relationship between the system nodes. Although the inputs of the model were time-series data, the model could not extract and accurately mine the temporal characteristics of the transient process. Reference [12] proposed a transient power angle stability assessment model based on a message-passing neural network (MPNN) that could describe the topological changes of power systems. However, the input feature quantity was steady-state data, which did not reflect the temporal characteristics of the transient process. Reference [13] established a deep forest (DF) model to solve the difficulties of evaluating the transient power angle stability caused by frequent topological changes in the power system. Although the spatial characteristics of the transient process were considered, the data after fault clearance were selected as inputs without considering the characteristics of the time-series data during the steady-state and fault processes.

In summary, even though the current transient power angle stability assessment methods primarily consider the spatiotemporal characteristics of the power system, they do not explore the spatiotemporal characteristics caused by changes in the network topology of the power system and changes in the relative power angle of the generators during the transient process.

In power systems, the faults occurring at different locations and times affect the transient power angle stability of the power system, and these faults have both spatial and temporal characteristics. When faults occur at different times, the operating state variables of the power system (e.g., the dynamic synchronous generator angle) exhibit significantly different time-series patterns and variations. These temporal characteristics can be used directly to assess the transient power angle stability of the power system. Similarly, when faults occur at different locations, the operating state variables of the power system exhibit different dynamic patterns and variations related to the locations of the faults. For example, the nodal voltage of a node near the fault location will have a large voltage drop, and synchronous generators within proximity of the fault location will have large variations in the power angle and electrical angular velocity [14]. Reference [15] discussed the effects of fault locations and times at which faults occurred on the transient power angle stability based on the spatiotemporal characteristics of the synchronous generator angles. The simulation results showed that the fault location affected the instability mode of the power system and lead-lag cluster of synchronous machines (spatial characteristics), whereas the moment at which the fault occurred affected the initial states of the generators (temporal characteristics), both of which had significant influence on the transient power angle stability. In brief, the time and location at which faults occur are the most important factors affecting the transient power angle stability [16], which emphasizes the need to consider spatiotemporal disturbance characteristics for transient power angle stability analysis. Hence, data-driven approaches should be capable of capturing these spatiotemporal characteristics to accurately assess the transient power angle stability of power systems.

Reference [17] used graph convolution network (GCN) and long short-term memory (LSTM) network to extract spatiotemporal features from massive data for short-term load forecasting. Reference [18] proposed a disturbance-after-frequency prediction method based on the GCN-LSTM model for power system frequency forecasting. Reference [19] designed a GCN and LSTM-based voltage stability prediction method to handle complex dynamic characteristics for online short-term voltage stability analysis. These studies demonstrate the potential of the GCN-LSTM model to tackle various problems. However, the application of the GCN-LSTM model for transient power angle stability assessment has never been reported, and therefore, it is deemed essential to design a transient power angle stability assessment method based on the GCN-LSTM model to explore the spatiotemporal disturbance characteristics of future power systems.

Thus, in this study, a new GCN-LSTM model is proposed for transient power angle stability assessment based on the spatiotemporal disturbance characteristics of power systems. LSTM networks, which are capable of capturing temporal dependencies, face limitations in effectively grasping the spatial characteristics inherent within graph-structured data. This is where GCN comes into play, complementing the shortcomings of the

LSTM network. GCNs excel in capturing the spatial features of graphs by leveraging the connectivity and relationships between nodes and edges (e.g., buses and lines in a power system). This capability allows GCNs to understand and incorporate the structural information of the power grid, such as the physical connections between different components and their influence on each other, which is crucial to accurately assess the transient power angle stability of the power system. In this study, first, the GCN model is used to extract the spatial characteristics, and these characteristics are used in the LSTM model to obtain the temporal characteristics. The spatial changes in the network topology and the temporal changes in the electrical state quantities are fused through a fully connected network to determine the spatiotemporal disturbance characteristics of the power system. Finally, simulations are performed to verify the accuracy and effectiveness of the proposed transient power angle stability assessment model based on the spatiotemporal characteristics. The main contributions of this study are as follows.

1) A GCN-LSTM model is proposed to assess the transient power angle stability by extracting the spatial changes in the network topology and temporal changes of electrical state quantities during transient processes. The proposed model outperformed the LSTM [6], 1D-CNN [20], 1D-CNN-LSTM [21], and GCN [22] models in terms of the accuracy, recall rate, and training and testing times for transient power angle stability analysis of three practical power systems.

2) The accuracy of the GCN-LSTM model with different number of iterations and LSTM layers is also explored and compared with other models. The simulation results verify that the GCN-LSTM model is non-sensitive to the number of iterations and LSTM layers.

The remainder of this paper is organized as follows. The GCN-LSTM model is described in detail in Section II. Section III presents the transient power angle stability assessment model based on GCN and LSTM network. Section IV presents the simulations of a hybrid AC-DC practical power system used to verify the proposed GCN-LSTM model. The performance metrics of the GCN-LSTM model with different number of iterations and LSTM layers are analyzed and compared with those of the other models. Finally, the conclusions of this study are presented in Section V.

II. GCN-LSTM Model

A. Extraction of Spatial Characteristics Based on GCN

To obtain the spatial characteristics generated by changes in the topological structure of a power system network, a GCN can be used to transform the network topology into a graph structure and extract the spatial characteristics. The graph structure $\boldsymbol{G}=(\boldsymbol{X}_G,\boldsymbol{A})$ contains N nodes. Each node has M features, and the features of all nodes can form an $N\times M$ dimensional feature matrix $\boldsymbol{X}_G$. $\boldsymbol{A}$ is the $N\times N$ dimensional adjacency matrix that describes the topological relationship between the system nodes [23]. A GCN model can be used to aggregate the power system topology and node information to obtain the spatial characteristics, including the original feature and connection information.

In the adjacency matrix $\boldsymbol{A}=(V,E)$, V is the set of nodes in the graph and E is the set of nodes connected to the edges. The element A_{ij} in the adjacency matrix $\boldsymbol{A}$ can be determined based on whether the nodes (V_i,V_j) are connected (i.e., whether there are edges). The elements A_{ij} can be determined from

$$A_{ij}=\begin{cases}0, & (V_i,V_j)\notin E\\ 1, & (V_i,V_j)\in E\end{cases} \tag{1}$$

where (V_i,V_j) represents the connected edges of the nodes i and j. Further transformation of the adjacency matrix $\boldsymbol{A}$ is necessary because it does not consider the information of the node itself, but only the connections with other nodes. The transformation of the adjacency matrix $\boldsymbol{A}$ is given by

$$\tilde{\boldsymbol{A}}=\boldsymbol{A}+\boldsymbol{I} \tag{2}$$

where $\boldsymbol{I}$ represents an $N\times N$ dimensional identity matrix. The more edges a node is connected to, the more it is affected by neighboring nodes because each node is connected to other nodes differently. Therefore, each node has different influencing weights on the surrounding nodes, which can be expressed through the degree matrix $\tilde{\boldsymbol{D}}$ as

$$\tilde{D}_{ii}=\sum\nolimits_j \tilde{A}_{ij} \tag{3}$$

where $\tilde{D}_{ii}$ is an element of $\tilde{D}$ and $\tilde{A}_{ij}$ is an element of the adjacency matrix $\tilde{\boldsymbol{A}}$. Extracting the corresponding spatial characteristics is necessary to explore the spatial characteristics of the network topology. The spatial characteristics can be extracted using a GCN model based on the initial feature matrix $\boldsymbol{X}$. The model is expressed as

$$H^{(l+1)}=\sigma_{\text{sigmoid}}(\tilde{\boldsymbol{D}}^{-\frac{1}{2}}\tilde{\boldsymbol{A}}\tilde{\boldsymbol{D}}^{-\frac{1}{2}}H^{(l)}W^{(l)}) \tag{4}$$

where σ_{sigmoid} is the activation function; $H^{(l)}$ is the spatial characteristic extracted from the l layer of the GCN model ($H^{(l)}\in R^{N\times M}$, $H^{(0)}=X$); $\boldsymbol{W}^{(l)}$ is the weight matrix of the l layer, which is the parameter to be trained. $\boldsymbol{W}^{(l)}\in R^{M\times\alpha}$ and a are the spatial characteristic dimensions of the output. Thus, $H^{(l+1)}\in R^{N\times\alpha}$.

B. Extraction of the Temporal Characteristics Based on LSTM

Owing to the transient processes in power systems, where electrical state quantities such as generator power angles, bus voltages, and phase angles vary over time as

time-series data with temporal characteristics, the LSTM model is selected to extract the temporal features.

Each LSTM unit contains input, output, and forgetting gates, as listed in Table I [24]–[26].

TABLE I
INPUT AND OUTPUT DIMENSIONS OF THE GCN-LSTM MODEL

Layer	Input dimensions	Output dimensions
GCN	(b,N,T,M)	(b,N,T,α)
LSTM	$(b,T,N\times\alpha)$	(b,T,β)
FC	(b,T,β)	(b,ε)

The forgetting gate linearly transforms the input x_t at time t with the output h_{t-1} at time $t-1$ and is obtained by activating the function f_t via σ.

$$f_t=\sigma(W_f\cdot[h_{t-1},x_t]+b_f) \tag{5}$$

where f_t is the output value of the forgetting gate; x_t is the input at time t; h_{t-1} is the output at time $t-1$; $[h_{t-1},x_t]$ is the integration of h_{t-1} and x_t; W_f is the weight parameter of the forgetting gate; b_f is the offset of the forgetting gate; and σ is the sigmoid activation function.

The input gate first selects the upper layer information x_t, h_{t-1} through the sigmoid activation function to obtain i_t. To obtain the input state $\tilde{C}_t$ at time t, a tanh activation function is selected to reselect the upper layer information. Finally, the internal state C_{t-1} at time $t-1$ is updated to the internal state C_t at time t. These operations are expressed as

$$i_t=\sigma_{\text{sigmoid}}(W_i\cdot[h_{t-1},x_t]+b_i) \tag{6}$$

$$\tilde{C}_t=\sigma_{\tanh}(W_{\text{c}}\cdot[h_{t-1},x_t]+b_{\text{c}}) \tag{7}$$

$$C_t=f_t\times C_{t-1}+i_t\times\tilde{C}_t \tag{8}$$

where i_t denotes the output value of the input gate; W_i denotes the weight parameter of the input gate; b_i denotes the offset of the input gate; σ_{sigmoid} denotes the sigmoid activation function; $\tilde{C}_t$ is the input state at time t; W_{c} is the weight parameter of the input state; b_{c} is the bias term of the input state; and $\sigma_{\tanh}$ is the tanh activation function; C_t is the internal state at time t and C_{t-1} is the internal state at time $t-1$.

The output gate controls the output at time t, which first determines the output value o_t of the output gate through the sigmoid activation function and then combines the internal state C_t at time t to obtain the final output h_t. The equations to determine o_t and h_t are given by

$$o_t=\sigma(W_{\text{o}}\cdot[h_{t-1},x_t]+b_{\text{o}}) \tag{9}$$

$$h_t=o_t\times\sigma_{\tanh}(C_t) \tag{10}$$

where o_t is the output value of the output gate; W_{o} is the weight parameter of the output gate; b_{o} is the offset term of the output gate; h_t is the output at time t with temporal characteristics ($h_t\in R^{T\times\beta}$); T is the dimension of the input data time series; and β is the output temporal characteristic dimension (i.e., the number of neurons in the hidden layer). Figure 1 shows the internal structure of the LSTM network.

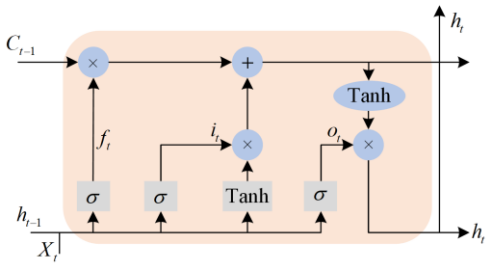

Fig. 1. Schematic of the internal structure of the LSTM network.

C. Extraction of the Spatiotemporal Characteristics Based on the GCN-LSTM Model

Based on the network and graph theory, the network topology of a power system can be regarded as a graph structure [27], where each generator is represented by a node in the graph structure, the connecting lines between the generators are represented by the edges in the graph structure, and the power angles of the generators, nodal voltages, and phase angles in the transient process are the characteristic quantities of each node. Owing to the different connection modes between the generator nodes, the neighboring nodes affect each node differently, and different spatial characteristics are generated during the transient process. Moreover, the characteristic quantities of the generator nodes are a continuous time-series data with temporal characteristics. Therefore, to assess the transient power angle stability of power systems, considering the spatiotemporal disturbance characteristics, a GCN-LSTM model is proposed in this study, that integrates the spatiotemporal characteristics, as listed in Table II.

TABLE II
CONFUSION MATRIX OF THE TRANSIENT POWER ANGLE STABILITY ASSESSMENT

	Stability prediction	Instability prediction
Stability	T_{P}	F_{N}
Instability	F_{P}	T_{N}

First, the GCN model is used to extract the spatial characteristics, and these characteristics are used as the inputs for the LSTM model to extract the temporal characteristics. Subsequently, the characteristics are fused through a fully connected layer (FC) to obtain the spatiotemporal characteristics. The transient power angle stability assessment problem can be regarded as a binary classification problem, and thus, the softmax

activation function is used to calculate the probability of the sample being stable or unstable as the predicted value. The labels for the stable and unstable samples are set at 0 and 1, respectively. Finally, the error between the predicted and true values is calculated using the loss function [28] and reduced by updating the model weight and bias parameters to obtain the optimal model.

The structure of the GCN-LSTM model is as follows: 1-layer GCN + 4-layer LSTM + 1-layer FC + softmax activation function. The input of the model includes the initial feature matrix $\boldsymbol{X}=\{x_0, x_1 \cdots x_T\}$ $(X \in R^{b\times N\times T\times M})$, the adjacency matrix $\boldsymbol{A}$ $(\boldsymbol{A} \in R^{N\times N})$, and the true value y $(y \in R^b)$. Here, b is the number of data samples for batch training, N is the number of nodes, and T is the dimension of the input data time series. M is the dimension of the node features, and the output of the model consists of the predicted values $\hat{y}$ $(\hat{y} \in R^{b\times 2})$.

The GCN layer first extracts the spatial features from the initial feature matrix $\boldsymbol{X}$. The dimensions of the input data $\boldsymbol{X}$ and output space are (b,N,T,M) and (b,N,T,α), respectively, and a is the number of spatial features. Because the features of all nodes can be regarded as a whole when the temporal features are extracted, the input data of the LSTM layer are transformed from the output dimension (b,N,T,α) of the GCN layer to the dimension $(b,T,N\times\alpha)$. The dimensions of the output time feature h_t are (b,T,β), where β is the number of temporal features. The data outputted by the LSTM are fused through the FC layer to obtain the spatiotemporal characteristics. Because the value h_T $(h_T \in R^{(b,\beta)})$ only needs to be selected to determine the temporal characteristics at the last moment during the fusion of the FC layer, the input dimension of the FC layer is (b,T,β), the output dimensions are (b,ε), and ε is the number of spatiotemporal characteristics. The final two-dimensional (2D) features must be obtained because the transient power angle stability assessment is a binary classification problem (i.e., $\varepsilon = 2$), as shown in Table I. Figure 2 shows the internal structure of the GCN-LSTM model.

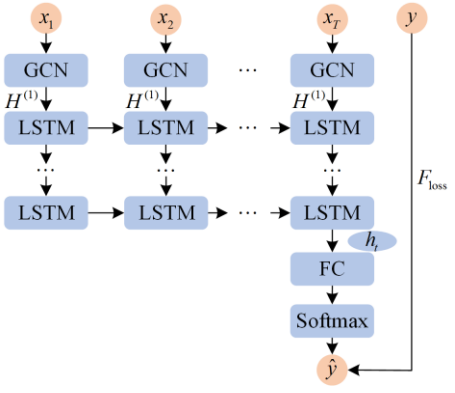

Fig. 2. Schematic of the internal structure of the GCN-LSTM model.

The obtained 2D spatiotemporal characteristics are mapped to a probability value between 0 and 1 using the softmax activation function (i.e., the predicted value $\hat{y}=\{p_1, p_2\}$. $\hat{y}$ can be used as a basis for judging the sample instability, and the true value of y is the label of the data sample for batch training. In this study, the cross-entropy loss function [29] is used to compute the error between the predicted value $\hat{y}$ and true value y, which is expressed as

$$F_{\text{loss}} = -[y \log p_1 + (1-y)\log p_2] \tag{11}$$

where p_1 is the probability of predicting the sample instability (labeled 1), p_2 is the probability of predicting the sample stability (labeled 0), and $p_2 = 1 - p_1$.

III. Proposed GCN-LSTM Model for Transient Power Angle Stability Assessment

A. Input Feature Quantities

Constructing a reasonable initial feature matrix $\boldsymbol{X}$ as the input of the GCN-LSTM model is necessary to effectively evaluate the transient power angle stability of the power system and use the spatiotemporal disturbance characteristics during the transient process. Therefore, considering a single sample as an example, $\boldsymbol{X} \in R^{N\times T\times M}$, where N is the number of nodes in the network topology, the conventional generator set in the power system is selected as the node in this study. Here, M is the dimension of the node features, and each node contains three features: relative power angle of the generator $\Delta\delta$, bus voltage amplitude of the generator U, and phase angle θ. Hence, $M = 3$. T is the dimension of the input data time series. To fully consider the transient characteristics of the power system from steady-state to fault occurrence to fault removal T_{w}, a continuous time series W is selected, encompassing three periods: from steady-state time to fault occurrence time t_{f}, from fault occurrence time t_{f} to fault removal time t_{c}, and fault removal time, as shown in Fig. 3.

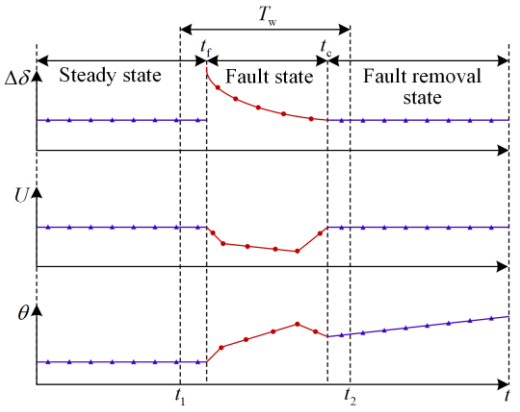

Fig. 3. Continuous time series of the transient power angle stability fault.

The sampling interval is set as D. T_{w} is the time series including the steady-state period, the fault period, and the three periods after fault excisions. The interval is $[t_1, t_2]$ and $T = \dfrac{T_{\mathrm{w}}}{D}$ is the dimension of the input data time series (i.e., the number of sampling points in the period T_{w}). Therefore, by taking a sample as an example, the input data of the relative power angle of the generator $\Delta\delta$, bus voltage amplitude of the generator U, and phase angle θ are all $T \times N$ dimensional data, which can be expressed as

$$\Delta\delta = \begin{bmatrix} \Delta\delta_{1,1} & \Delta\delta_{1,2} & \cdots & \Delta\delta_{1,N} \\ \Delta\delta_{2,1} & \Delta\delta_{2,2} & \cdots & \Delta\delta_{2,N} \\ \vdots & \vdots & & \vdots \\ \Delta\delta_{T,1} & \Delta\delta_{T,2} & \cdots & \Delta\delta_{T,N} \end{bmatrix} \tag{12}$$

$$U = \begin{bmatrix} U_{1,1} & U_{1,2} & \cdots & U_{1,N} \\ U_{2,1} & U_{2,2} & \cdots & U_{2,N} \\ \vdots & \vdots & & \vdots \\ U_{T,1} & U_{T,2} & \cdots & U_{T,N} \end{bmatrix} \tag{13}$$

$$\theta = \begin{bmatrix} \theta_{1,1} & \theta_{1,2} & \cdots & \theta_{1,N} \\ \theta_{2,1} & \theta_{2,2} & \cdots & \theta_{2,N} \\ \vdots & \vdots & & \vdots \\ \theta_{T,1} & \theta_{T,2} & \cdots & \theta_{T,N} \end{bmatrix} \tag{14}$$

where $\Delta\delta_{T,N}$, $U_{T,N}$, and $\theta_{T,N}$ are the relative power angle, bus voltage, and phase angle of N generators at the sampling point T, respectively.

B. Data Preprocessing

To prevent convergence problems caused by large numerical differences between features, the Z-score is used to normalize all of the feature data x in the initial feature matrix $\boldsymbol{X}$ [30], which is given by

$$\bar{x} = \frac{x - \mu_x}{\sigma_x} \tag{15}$$

where $\bar{x}$ is the characteristic data normalized by x; μ_x is the mean value of data x; and σ_x is the standard deviation of data x.

C. Performance Metrics of the Proposed GCN-LSTM Model

The transient power angle stability was determined using the transient stability index (TSI) [31], which is given by

$$M_{\mathrm{TSI}} = \frac{360° - \left|\Delta\delta_{\max}\right|}{360° + \left|\Delta\delta_{\max}\right|} \tag{16}$$

where $\Delta\delta_{\max}$ is the maximum relative power angle difference between any two generators during operation. When $M_{\mathrm{TSI}} > 0$, the system is stable. In contrast, when $M_{\mathrm{TSI}} < 0$, the system is temporarily unstable. According to the simulation results, the labels 0 and 1 denote the stable and unstable samples, respectively. Since the transient power angle stability assessment can be perceived as a binary classification problem, a confusion matrix [32] can be defined to evaluate the classification of the model, as shown in Table II. Here, T_{P} and T_{N} denote the number of correctly predicted stable and unstable samples, respectively, whereas F_{N} and F_{P} denote the number of stable and unstable samples with prediction errors, respectively.

A comparative analysis is conducted based on the accuracy and recall indices to determine the advantages and disadvantages of the GCN-LSTM model. The accuracy is defined as the proportion of the correctly predicted samples to the total number of samples [33], which is expressed as

$$R_{\mathrm{accuracy}} = \frac{T_{\mathrm{P}} + T_{\mathrm{N}}}{T_{\mathrm{P}} + F_{\mathrm{P}} + F_{\mathrm{N}} + T_{\mathrm{N}}} \tag{17}$$

The recall rate is defined as the proportion of samples with correct predictions in a few types of samples and is determined from

$$R_{\mathrm{recall}} = \frac{T_{\mathrm{N}}}{F_{\mathrm{P}} + T_{\mathrm{N}}} \tag{18}$$

The number of unstable samples in the stable transient power angle sample set is less than that of the stable samples, and the misjudgment of the unstable samples can be reflected by the recall rate. The higher the recall rate, the lower the misjudgment of the unstable samples.

D. Assessment of the GCN-LSTM Model

Figure 4 shows the flow chart of the transient power angle stability assessment of the power system based on the spatiotemporal disturbance characteristics. First, the initial feature matrix $\boldsymbol{X}$ with spatiotemporal information under different operation modes is obtained from simulations in the time domain. All of the feature data x in $\boldsymbol{X}$ and the corresponding labels (real values C) are used as the inputs for the GCN-LSTM model. The feature data are normalized using the Z-score, and the normalized feature data $\bar{x}$ and label y are randomly divided into training and testing sets. The GCN-LSTM model is trained using the training set. Conventional thermal power units in the system are considered as nodes in the graph structure. The adjacency matrix $\boldsymbol{A}$ is computed and inputted into the model according to the positional relationship and connection of each generator. The predicted values $\hat{y}$ are obtained using the trained GCN-LSTM model tested on the testing set. The model is classified according to its predicted values. Finally, the model is evaluated according to the labels and performance metrics.

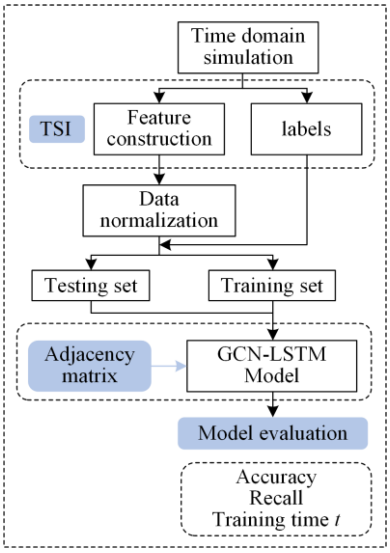

Fig. 4. Flow chart of the transient power angle stability assessment.

IV. Analysis of Numerical Examples

In this section, a modified 53-bus practical power system is used to test the proposed GCN-LSTM model, as shown in Fig. 5. In the system, four photovoltaic power stations with a total installed capacity of 1600 MW and eight wind generators with a total installed capacity of 3200 MW are bundled and connected via three AC lines and a 500 kV high-voltage direct current (HVDC) transmission line. Ten conventional thermal power units with a total capacity of 6000 MW are modeled as a 6th-order transient model with an IEEE type I excitation system. The parameters of the thermal power generators, HVDC transmission line, wind power generators, and photovoltaic systems are detailed in Tables A1 – A4 in the Appendix A.

The PSD-BPA power system simulation software is used to compute the power flow and temporary stability, adjust the load level to fluctuate between 80% and 120% of the original load, change the new energy simultaneity rates of 0%, 20%, 50%, and 60% for wind power harvesting stations A and B and photovoltaic power harvesting station C to obtain seven working conditions, and perform three-phase permanent N-1 failure on 26 lines. The fault location is set 25%, 50%, and 75% away from the first section of the line. The cycle time is 0.02 s, the sampling interval D is 0.01 s, the fault occurrence time t_f is the 50th cycle (1 s), and the fault removal time t_c is from the 57th cycle (1.14 s) to the 65th cycle (1.3 s), resulting in a total of nine occurrences. Owing to the different values of t_c, the selected time period T_w must include the fault removal time t_c under all working conditions to facilitate training and maintain the unity of the model input feature dimensions [34]. Therefore, the interval selected for T_w in this study is from the 49th cycle (0.98 s) to the 66.5th cycle (1.33 s)]. Thus, $T = 40$.

The transient power angle stability of the 4870 samples generated by the simulation software is determined according to the TSI, of which 3442 are stable and 1428 are unstable. The training and testing sets are randomly selected at a ratio of 7:3. By taking conventional generators as nodes in the graph structure with a total of 10 nodes, the adjacency matrix represents the connection matrix between these 10 generators, i.e., $\boldsymbol{A} \in \mathrm{R}^{10\times10}$. Therefore, the initial feature matrix $\boldsymbol{X} \in \mathrm{R}^{4870\times10\times40\times3}$ is constructed for all of the samples.

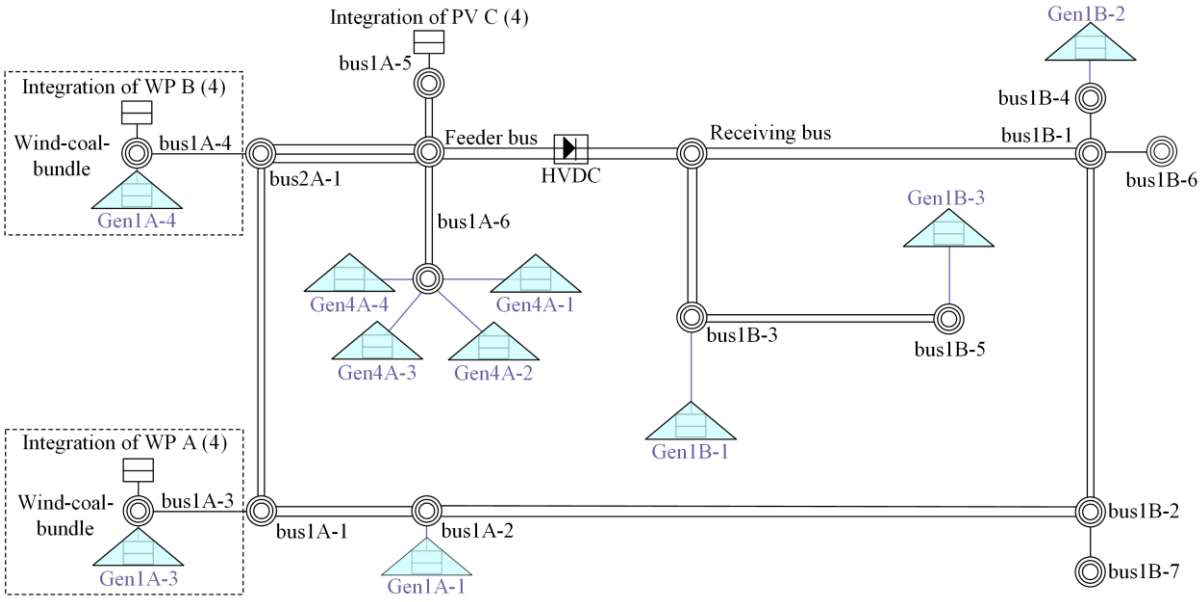

Fig. 5. Schematic of the modified 10-generator 53-bus practical power system.

A. Comparison of the Model Parameters and Algorithms

Pytorch 2.0.0 framework and Python programming language are used to verify the effectiveness of the GCN-LSTM model for transient power angle stability assessment, where Adam function is used as the training optimizer. The PC is configured with an Intel Core i5-12490F processor, 3.0 GHz central processing unit, 16 GB random access memory, and RTX 3060 12G graphics processing unit. The number of iterations, number of data samples for batch training, initial learning rate, number of spatial features, and number of temporal features are $N_{\text{epoch}}=100$, $b=64$, 0.0001, $\alpha=32$, and $\beta=32$, respectively.

By using a sample as an example, Fig. 6 shows the input and output dimensions of each layer. The dimensions of the input data $\boldsymbol{X}$ in the GCN layer are (10, 40, 3), and the dimensions of the output spatial features are (10, 40, 32). The dimensions of the input data of the LSTM layer and output temporal characteristics are (40, 10×32) and (40, 32), respectively. The output data of the LSTM layer are fused through the FC layer to obtain the spatiotemporal characteristics. The final 2D characteristics must be obtained because the transient power angle stability assessment is a binary classification problem. In other words, the input dimensions of the FC layer are (40, 32) and the output dimension is 2. Finally, the probability of a sample being stable or unstable (i.e., predicted value) is computed using the softmax activation function.

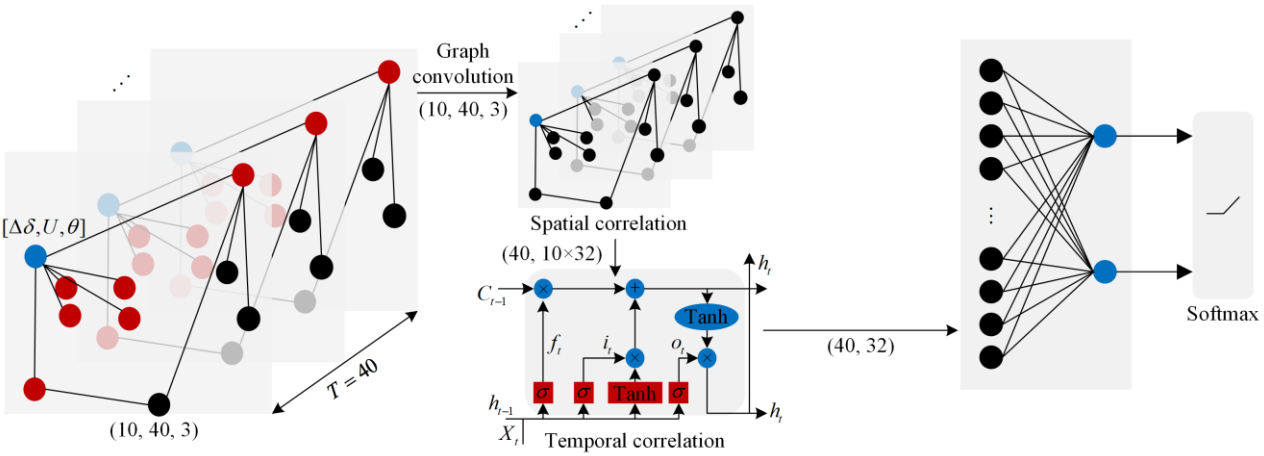

Fig. 6. Input and output dimensions of the GCN-LSTM model.

The GCN-LSTM model is compared with four other deep learning models: LSTM [6], 1D-CNN [20], 1D-CNN-LSTM [21], and GCN [22]. Based on the same system topology and parameter settings, the simulation results are obtained for the LSTM, 1D-CNN, 1D-CNN-LSTM and GCN models and compared with those of the proposed GCN-LSTM model. The GCN model is used to extract the spatial features, and the LSTM and 1D-CNN-LSTM models are used to extract the temporal characteristics. It shall be noted that the 1D-CNN model could not be used to extract the spatiotemporal characteristics. The structure of the GCN model is as follows: 1-layer GCN + 2-layer FC + softmax activation function. The input model dimensions are (64, 10, 40, 3), and the number of spatial features is $\alpha=32$. The structure of the LSTM model is as follows: 4-layer LSTM + 1-layer FC + softmax activation function. The input model dimensions are (64, 40, 10×3), and the number of temporal characteristics is $\beta=32$. The structure of the 1D-CNN model is as follows: 1-layer 1D-CNN + ReLU activation function + 1-layer pooled layer + 1-layer FC + softmax activation function. The input model dimensions are (64, 10×3, 40), the convolution kernel size is 3, the pool layer size is 3, and the number of convolutional layer output channels is 32. The structure of the 1D-CNN-LSTM model is as follows: 1-layer 1D-CNN + ReLU activation function + 1-layer pooling layer + 4-layer LSTM + 1-layer FC + softmax activation function. The input model dimensions are (64, 10×3, 40), and the parameters of the 1D-CNN-LSTM model are consistent with those of the 1D-CNN and LSTM models, which uses a cross-entropy loss function. The performance of the classifier is evaluated and compared based on four metrics (accuracy, recall rate, training time, and testing time), as shown in Table III. The training time refers to the total duration of training (100 epochs) for 3409 samples, and the testing time is the time required for transient power angle stability assessment of a single sample.

TABLE III
COMPARISON OF THE PERFORMANCE OF DIFFERENT DEEP LEARNING MODELS

Model	Accuracy (%)	Recall (%)	Training time (min)	Testing time (ms)
GCN	87.41	78.64	44.54	50.99
LSTM	87.81	70.80	59.56	52.29
1D-CNN	87.33	66.67	25.45	63.51
1D-CNN-LSTM	97.18	98.00	62.95	50.31
Proposed GCN-LSTM	98.59	98.32	24.32	43.26

Table III shows that the accuracy of the GCN-LSTM model is about 11% higher than that of the GCN, LSTM and 1D-CNN models, and it is slightly better than the accuracy of the 1D-CNN-LSTM model. By comparing the data in column 3 of Table III, the GCN-LSTM model also has the highest recall rate, which is 20%, 28%, and 32% higher than those of the GCN, LSTM, and 1D-CNN models. The training time of GCN-LSTM model is 24.32 min, which is significantly lower than those of the GCN, LSTM, 1D-CNN, and 1D-CNN-LSTM models. Furthermore, the proposed GCN-LSTM model is capable of performing transient power angle stability assessment within 43.26 ms, which is significantly faster than other models. Because the 1D-CNN model could not extract the spatiotemporal characteristics, its accuracy and recall rate are lower than those of other models. Furthermore, compared with the GCN and LSTM models, the hybrid GCN-LSTM and 1D-CNN-LSTM models has higher accuracy, better recall rate, faster evaluation time, and shorter training time. The proposed GCN-LSTM model is superior to other models tested in this study since it exploits the spatiotemporal data mining capability of GCN and LSTM and effectively extracts comprehensive characteristics from the training data.

To verify the generalization capability of the proposed model, three power systems are tested. System 1 is a modified 10-generator 53-bus practical power system, as shown in Fig. 5. As shown in Fig. 7, System 2 is a 100-bus practical power system with 11 synchronous generators, 6 photovoltaic systems, and 6 wind farms, with an installed capacity of 6300 MW, 600 MW, and 2400 MW, respectively. System 3 is a 197-bus practical power system that consists of 18 generators, 12 photovoltaic systems, and 12 wind farms with a total capacity of 9800 MW, 2400 MW, and 2400 MW, respectively, and four DC lines, as shown in Fig. 8. The same sample generation scheme is employed for all of these systems, and the validation results are summarized in Table IV.

TABLE IV
PERFORMANCE OF THE GCN-LSTM MODEL FOR DIFFERENT POWER SYSTEMS

Power system	Accuracy (%)	Recall (%)	Training time (min)	Testing time (ms)
53-bus system	98.59	98.32	24.32	43.26
100-bus system	97.95	94.15	28.11	45.08
197-bus system	98.97	97.64	32.45	46.17

It is evident from Table IV that the proposed GCN-LSTM model exhibits robust performance when it is tested on different power systems. The training and testing times for the 10-generator 53-bus system are 24.32 min and 43.26 ms, respectively. The training and testing times slightly increase with an increase in the system size and expansion of the dataset dimensions; however, they do not affect the overall effectiveness of the GCN-LSTM model. In general, the maximum training time is 32.45 min and the testing time do not exceed 47 ms for these three power systems, proving the universality of the proposed model.

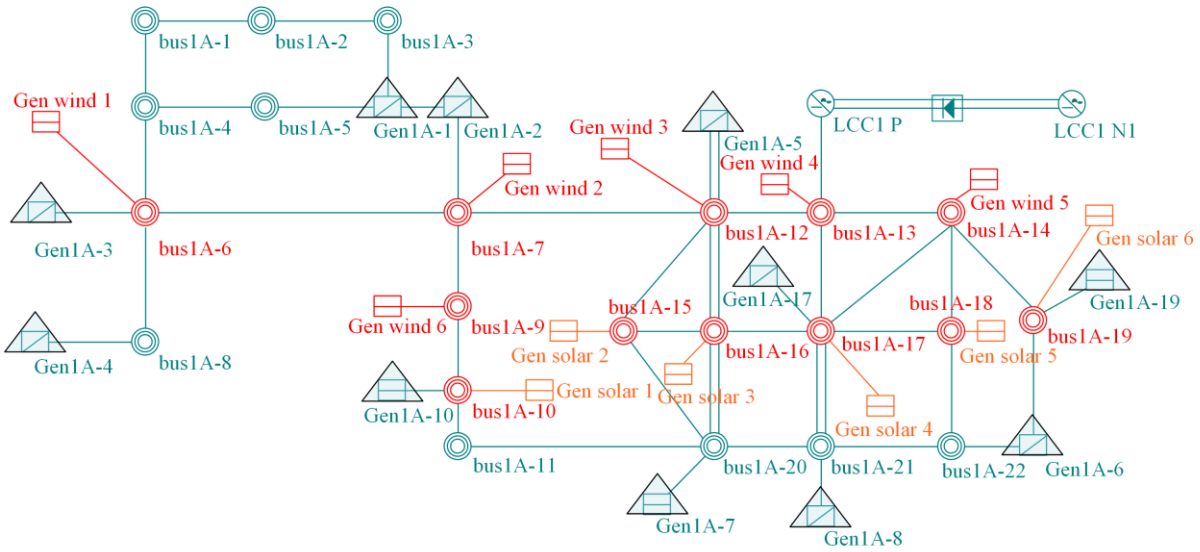

Fig. 7. Schematic of the modified 11-generator 100-bus practical power system.

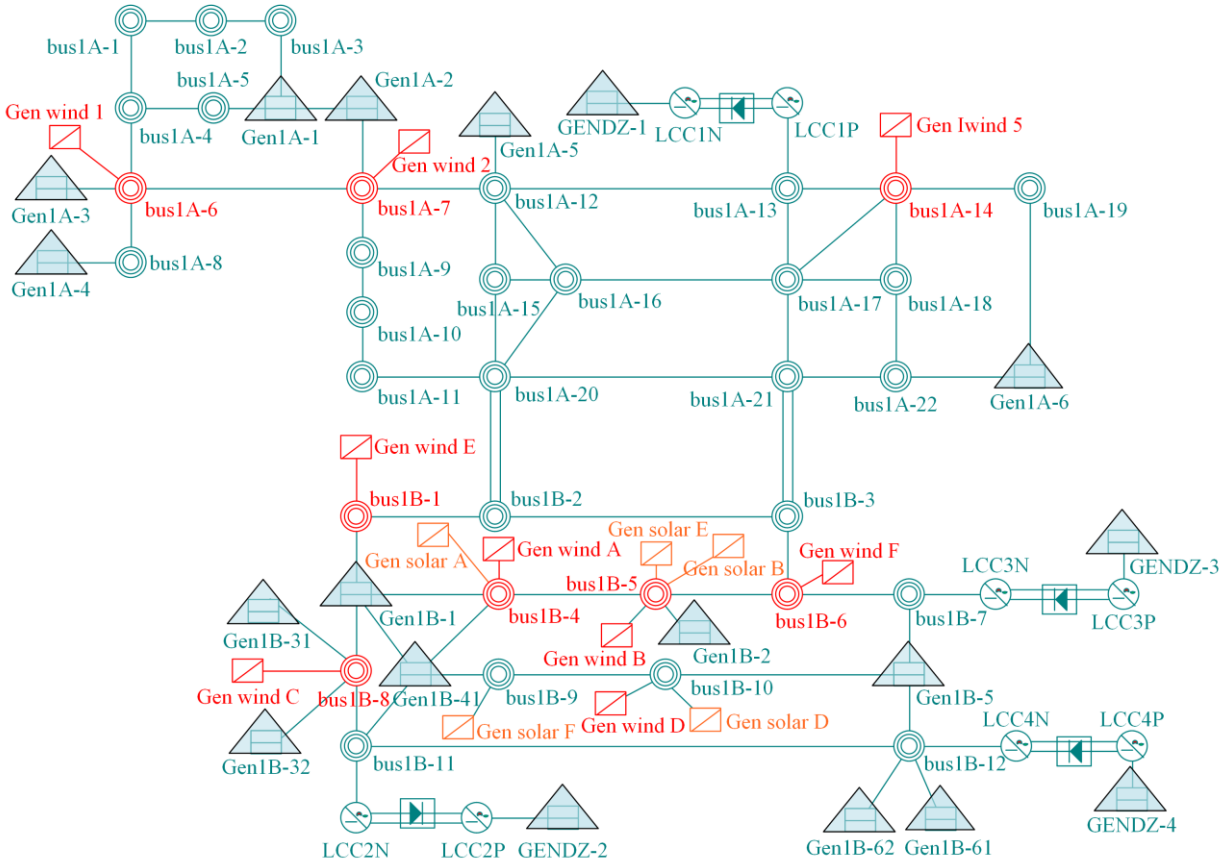

Fig. 8. Schematic of the modified 18-generator 197-bus practical power system.

B. Effect of the Number of Iterations on Different Deep Learning Models

As shown in Fig. 9, the accuracy of the testing set for each model gradually increased as the number of iterations (epoch) increased. However, the accuracy stabilized when the training reached the 100th cycle, indicating that the number of iterations is not optimal. The performance of the models is stabilized after reaching a particular value. Continuous training of the models result in overfitting of the models.

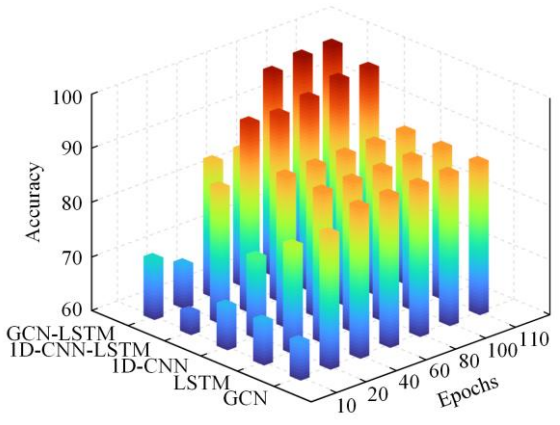

Fig. 9. Relationship between the accuracy of the testing set and number of iterations for the transient power angle stability assessment models.

C. Effect of the Number of LSTM Layers on the GCN-LSTM Model

To verify the effect of the number of LSTM layers on the accuracy, recall rate, and training time for one epoch, GCN-LSTM models with 1–5 LSTM layers (denoted as A–E) are denoised and the results are compared, as shown in Fig. 10. It can be observed that the accuracy and recall rate of the GCN-LSTM model are significantly increased with an increase in the number of LSTM layers. However, the accuracy and recall rate of the model with five LSTM layers are decreased, indicating that overfitting occurred when the number of layers exceeded a particular value. Therefore, increasing the number of LSTM layers in the GCN-LSTM model did not necessarily improve performance of the model, and other performance parameters must be considered.

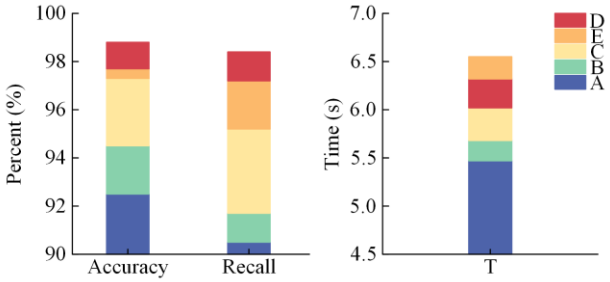

Fig. 10. Relationship between the number of LSTM layers and the performance metrics of the GCN-LSTM model.

V. Conclusion

In this study, a transient power angle stability assessment method based on the GCN-LSTM model is proposed to accurately analyze the transient power angle stability of future power systems, considering spatiotemporal disturbance characteristics. First, the GCN obtains the spatial characteristics in the system network topology, and the LSTM network excavates the temporal characteristics in continuous time-series data, such as the relative power angle of the generators. The spatiotemporal characteristics are fused through the FC layer to perform transient power stability assessment. Finally, simulations are conducted using the model on a hybrid 500 kV AC-DC practical power system to verify the performance of the model. The following conclusions are drawn based on the key findings of this study.

1) By exploiting the advantages of the GCN and LSTM to extract the spatiotemporal disturbance characteristics, the proposed GCN-LSTM model for transient power angle stability assessment explores the temporal characteristics of the time-series relative power angle of the generators and the spatial characteristics of the node connection adjacency matrix. Therefore, the proposed model can effectively evaluate the transient power angle stability of power systems.

2) Compared with the GCN, LSTM, 1D-CNN, and 1D-CNN-LSTM models, the proposed GCN-LSTM model achieves the highest accuracy and recall rate for the transient power angle stability assessment with the cheapest computational cost, as indicated by the training and testing times.

3) The accuracy of the GCN-LSTM model is investigated by varying the number of iterations and number of LSTM layers, and the simulation results show that the performance of the GCN-LSTM model is stabilized and nonsensitive to these parameters once they reach a certain threshold.

However, there are some shortcomings with the proposed GCN-LSTM model, which need to be addressed in the future, as follows:

1) The proposed GCN-LSTM model only considers the transient power angle stability assessment as a binary classification problem without quantifying the stability margin. The next step is to refine the relationship between the stability margin and transient feature quantities.

2) The proposed GCN-LSTM model consists of only a single layer in the GCN without considering the effect of multiple layers of the GCN on the model performance. In the future, a multilayer GCN-LSTM model will be developed for a more comprehensive transient power angle stability assessment.

Appendix A

TABLE A1
Parameters of the Thermal Power Generators

Parameter	Value
Maximum generator power (MW)	600
d-axis synchronous reactance (p.u.)	1.918
d-axis transient reactance (p.u.)	0.284
d-axis subtransient reactance (p.u.)	0.218
q-axis synchronous reactance (p.u.)	1.867
q-axis transient reactance (p.u.)	0.428
q-axis subtransient reactance (p.u.)	0.217
d-axis transient time constant (s)	7.880
q-axis transient time constant (s)	0.870
d-axis subtransient time constant (s)	0.046
q-axis subtransient time constant (s)	0.070
Inertia time constant (s)	14.993

TABLE A2
Parameters of the Wind Power Generators

Parameter	Value
Air density (kg/m^3)	1.390
Turbine blade radius (m)	35.200
Turbine blade rotational speed (rpm)	15.400
Turbine rated wind speed (m/s)	11.800
Shaft stiffness coefficient (Nm/rad)	8.87×10^7
Shaft damping coefficient (Nm/rad)	2.5×10^5
Maximum generator power (MW)	400
Generator stator inductance (p.u.)	0.086
Generator rotor inductance (p.u.)	0.095
Generator mutual inductance (p.u.)	4.100
Generator stator resistance (p.u.)	0.010
Generator rotor resistance (p.u.)	0.009
Generator rated speed (rpm)	1500

TABLE A3
Parameters of the Photovoltaic Systems

Parameter	Value
Reference cell temperature (°C)	15
Reference illumination intensity (W/m^2)	1000
Maximum power of photovoltaic array (MW)	400

TABLE A4
Parameters of the HVDC Transmission Line

Parameter	Value
Rectifier-side DC reference voltage (kV)	210
Inverter-side DC reference voltage (kV)	199
Number of rectifiers and inverters (2)	2
Rated DC transmission line current (A)	5000
DC circuit resistance (Ω)	5
DC active power (MW)	500
DC voltage (kV)	500
Rectifier-side normal firing angle (°)	15
Inverter-side normal extinction angle (°)	17

Acknowledgment

Not applicable.

AUTHORS' CONTRIBUTIONS

Shiwei Xia: conceptualization, validation, writing-review & editing. Chenhui Zhang: conceptualization, methodology, software, formal analysis. Yahan Li: investigation, data curation, writing-original draft. Gengyin Li: writing-review & editing, funding acquisition, project administration. Linlin Ma: validation, writing-review & editing, funding acquisition. Ning Zhou: writing-review & editing, project administration. Ziqing Zhu: conceptualization, writing-review & editing. Huan Ma: review & editing, funding acquisition.

FUNDING

This work is supported by the National Key R&D Program of China "Response-driven Intelligent Enhanced Analysis and Control for Bulk Power System Stability" (No. 2021YFB2400800 and No. SGSDDKOOWJJS 2200092).

AVAILABILITY OF DATA AND MATERIALS

Not applicable.

DECLARATIONS

Competing interests: The authors declare that they have no known competing financial interests or personal relationships that could have appeared to influence the work reported in this article.

AUTHORS' INFORMATION

Shiwei Xia received the Ph.D. degree in power systems from the Hong Kong Polytechnic University, Hong Kong, China in 2015, where he then worked as a research associate and subsequently as a postdoctoral fellow in 2015 and 2016. He was also a visiting faculty with the Robert W. Galvin Center for Electricity Innovation, Illinois Institute of Technology, Chicago, IL, USA, in 2019. Currently, he is with the School of Electrical and Electronic Engineering, North China Electric Power University, Beijing, China. His general research interests include security and risk analysis for power systems with renewable energies, distributed optimization and control of multiple sustainable energy sources in smart grid.

Chenhui Zhang received the B.S. degrees in electrical engineering from Tianjin University of Technology, Tianjin, China, in 2022. He is currently pursuing the Ph.D. degree in electrical engineering at North China Electric Power University. His research interests include security and risk analysis for power systems with renewable energies.

Yahan Li received the B.S. degree in electrical engineering from China Three Gorges University, Yichang, Hubei, in 2021 and the M.S. degree in electrical engineering from North China Electric Power University, Beijing, China, in 2024. Her research interest includes transient power angle stability.

Gengyin Li received the B.S., M.S. and Ph. D. degrees, in electrical engineering from North China Electricity Power University in 1984, 1987, and 1996 respectively. Since 1987, Dr. Li has been with the School of Electrical and Electronic Engineering at North China Electric Power University, where he is currently a professor. His areas of interest include HVDC transmission, power quality analysis and control, and new transmission and distribution technologies.

Linlin Ma received the Ph.D. degree in power system and automation from Shandong University, Jinan, China, in 2010. Her research interests include the stability and control of new-type power system, active support of new energy plants.

Ning Zhou received the B.S. and M.S. degrees, in electrical engineering from Zhejiang University in 2010 and 2014 respectively. Since 2014, she has been working at State Grid Shandong Electric Power Research Institute. Her areas of interest include power system analysis, power system simulation and modeling methods of renewable energy stations.

Ziqing Zhu received the M.S. degree in electrical power systems engineering from the University of Manchester, U.K., in 2019, and the Ph.D. degree from the Hong Kong Polytechnic University, Hong Kong, SAR, China, in 2023. He is currently a research assistant professor with the Department of Computer Science, Hong Kong Baptist University. He is serving as the early career researcher associate editor of IET Smart Grid. His research interests include applications of artificial intelligence and machine learning in power system operation and power markets.

Huan Ma received the Ph.D. degree in power system and automation from Shandong University, Jinan, China, in 2017. He is currently a senior engineer in State Grid Shandong Electric Power Research Institute. His research interests include the stability and control of new-type power system, active support of new energy plants.

REFERENCES

[1] Z. Zhong, L. Guan, and Y. Su *et al*., "Power system transient stability assessment based on graph attention deep network," *Power System Technology*, vol. 45, no. 6, pp. 2122-2130, Jun. 2021. (in Chinese)

[2] L. Ji, J. Wu, and Y. Zhou *et al*., "Using trajectory clusters to define the most relevant features for transient stability

prediction based on machine learning method," *Energies*, vol. 9, no. 11, Nov. 2016.

[3] X. Qiao, Z. Wang, and Z. Li, "Transient stability assessment for AC-DC hybrid systems based on Bayesian optimization XGBoost," in *2022 International Conference on Power Energy Systems and Applications (ICoPESA)*, Singapore, Singapore, Feb. 2022, pp. 219-224.

[4] Y. Zhou, J. Wu, and L. Hao *et al*., "Transient stability prediction of power systems using post-disturbance rotor angle trajectory cluster features," *Electric Power Components and Systems*, vol. 44, no. 17, pp. 1879-1891, Sep. 2016.

[5] S. Plathottam, H. Salehfar, and P. Ranganathan, "Convolutional neural networks (CNNs) for power system big data analysis," In *2017 North American Power Symposium (NAPS)*, Morgantown, WV, USA, Sep. 2017, pp. 1-6.

[6] Y. Du and Z. Hu, "Power system transient stability assessment based on snapshot ensemble LSTM network," *Sustainability*, vol. 13, no. 12, Jun. 2021.

[7] Y. Zhou and Y. Yang, "Transient stability assessment using gated recurrent unit," in *2020 5th Asia Conference on Power and Electrical Engineering (ACPEE)*, Chengdu, China, Jun. 2020, pp. 560-564.

[8] L. Sun, J. Bai, and Z. Zhou *et al*., "Transient stability assessment of power system based on bi-directional long-short-term memory network," *Automation of Electric Power Systems*, vol. 44, no. 13, pp. 64-72. Jul. 2020. (in Chinese)

[9] Q. Chen, N. Lin, and S. Bu *et al*., "Interpretable time-adaptive transient stability assessment based on dual-stage attention mechanism," *IEEE Transactions on Power Systems*, vol. 38, no. 3, pp. 2776-2790, May 2022.

[10] Z. Lu, X. Shi, and C. He, "Transient stability assessment based on two-step improved one-dimensional convolutional neural networks with long and short time-series input," in *2023 International Conference on Power System Technology (PowerCon)*, Jinan, China, Sep. 2023, pp. 1-5.

[11] J. Huang, L. Guan, and Y. Su *et al*., "A topology adaptive high-speed transient stability assessment scheme based on multi-graph attention network with residual structure," *International Journal of Electrical Power & Energy Systems*, vol. 130, 2021.

[12] Z. Wang, L. Guan, and Y. Su *et al*., "Transient stability assessment of power system considering topological change: a message passing neural network-based approach," *Proceedings of the CSEE*, vol. 41, no. 7, pp. 2341-2350, Apr. 2021. (in Chinese)

[13] X. Li, C. Liu, and P. Guo *et al*., "Transient stability assessment of power system considering change in network topology," *Smart Power*, vol. 49, no. 12, pp. 59-65, Dec. 2021.

[14] R. Kamel, S. Alanzi, and Y. Al Hashemi, "Effect of photovoltaic penetration level and location on power system transient stability during symmetrical and unsymmetrical faults," *Sustainable Energy*, *Grids and Networks*, 2024.

[15] O. Noureldeen, M. Rihan, and B. Hasanin, "Stability improvement of fixed speed induction generator wind farm using STATCOM during different fault locations and durations," *Ain Shams Engineering Journal*, vol. 2, no. 1, pp. 1-10, Jan. 2011.

[16] P. Sauer and M. Pai, "Power system dynamics and stability," Englewood Cliffs, NJ, USA: Prentice-Hall, 1998.

[17] D. Huang, H. Liu, and T. Bi *et al*., "GCN-LSTM spatiotemporal-network-based method for post-disturbance frequency prediction of power systems," *Global Energy Interconnection*, vol. 5, no. 1, pp. 96-107, Jan. 2022.

[18] G. Wang, Z. Zhang, and Z. Bian *et al*., "A short-term voltage stability online prediction method based on graph convolutional networks and long short-term memory networks," *International Journal of Electrical Power & Energy Systems*, vol. 127, 2021.

[19] S. Rizvi, "Time series deep learning for robust steady-state load parameter estimation using 1D-CNN," *Arabian Journal for Science and Engineering*, vol. 47, no. 3, pp. 2731-2744, May 2022.

[20] G. Gong, N. K. Mahato, and H. He *et al*., "Transient stability assessment of electric power system based on voltage phasor and CNN-LSTM," in *2020 IEEE/IAS Industrial and Commercial Power System Asia (I&CPS Asia)*, Weihai, China, Jul. 2020.

[21] D. Lu, J. Ren, and J. Chen, "Power system transient stability assessment based on graph convolutional network," in *2021 IEEE 4th International Electrical and Energy Conference (CIEEC)*, Wuhan, China, May 2021, pp. 1-5.

[22] R. Hossain, Q. Huang, and Huang R, "Graph convolutional network-based topology embedded deep reinforcement learning for voltage stability control," *IEEE Transactions on Power Systems*, vol. 36, no. 5, pp. 4848-4851, Nov. 2021.

[23] J. Huang, L. Guan, and Y. Su *et al*., "Recurrent graph convolutional network-based multi-task transient stability assessment framework in power system," *IEEE Access*, vol. 8, pp. 93283-93296, Apr. 2020.

[24] N. Mahato, J. Dong, and N. Wang, "Electric power system transient stability assessment based on Bi-LSTM attention mechanism," *in 2021 6th Asia Conference on Power and Electrical Engineering (ACPEE)*, Chongqing, China, Apr. 2021, pp. 777-782.

[25] Q. Chen and H. Wang, "Time-adaptive transient stability assessment based on gated recurrent unit," *International Journal of Electrical Power & Energy Systems*, vol. 133, 2021.

[26] T. Tarif, A. Ladjici, and A. Tiguercha *et al*., "Power system transient assessment using deep learning LSTM algorithm," in *2022 IEEE International Conference on Electrical Sciences and Technologies in Maghreb (CISTEM)*, Tunis, Tunisia, Oct. 2022, pp. 1-6.

[27] L. Zhu and D.J. Hill, "Networked time series shapelet learning for power system transient stability assessment," *IEEE Transactions on Power Systems*, vol. 37, no. 1, pp. 416-428, Jan. 2022.

[28] Y. Liang, Y. Ren, and J. Yu *et al*., "Current trajectory image-based protection algorithm for transmission lines connected to MMC-HVDC stations using CA-CNN," *Protection and Control of Modern Power Systems*, vol. 8, no. 1, Jan. 2023, pp. 1-15.

[29] Y. Du and Z. Hu, "Power system transient stability

assessment based on snapshot ensemble LSTM network," *Sustainability*, vol. 13, no. 12, Dec. 2021.

[30] S. Cheng, Z. Yu, and Y. Liu *et al*., "Power system transient stability assessment based on the multiple paralleled convolutional neural network and gated recurrent unit," *Protection and Control of Modern Power Systems*, vol. 7, no. 3, pp. 1-16, Jul. 2022.

[31] C. Chen, Z. Liu, and S. Feng *et al*., "Universal approximation capability of broad learning system and its structural variations," *IEEE Transactions on Neural Networks and Learning Systems*, vol. 30, no. 4, pp. 1191-1204, Apr. 2019.

[32] B. Chen, Q. Wu, and M. Li *et al*., "Detection of false data injection attacks on power systems using graph edge-conditioned convolutional networks," *Protection and Control of Modern Power Systems*, vol. 8, no. 2, pp. 1-12, Apr. 2023.

[33] Z. Li, Z. Jiao, and A. He *et al*., "A denoising-classification neural network for power transformer protection," *Protection and Control of Modern Power Systems*, vol. 7, no. 4, pp. 1-14, Oct. 2022.

[34] F. Shi, J. Wu, and J. Ji *et al*., "Integrated advance assessment of power system transient voltage and transient angle stability based on deep learning," *Power System Technology*, vol. 47, no. 2, pp. 741-758, Feb. 2023. (in Chinese)